Indian J Phys
https://doi.org/10.1007/s12648-021-02221-y

ORIGINAL PAPER

Enhancement in magnetic parameters of $L1_0$-FeNi on Pd-substitution for permanent magnets

P Rani[1], R Singla[1], J Thakur[2], A H Reshak[3,4,5] and M K Kashyap[1,6]*

[1]Department of Physics, Kurukshetra University, Kurukshetra, Haryana 136119, India

[2]Government Sr. Sec. School, Mussimbal, Yamunanagar, Haryana 135003, India

[3]Physics Department, College of Science, University of Basrah, Basrah 61004, Iraq

[4]Department of Instrumentation and Control Engineering, Faculty of Mechanical Engineering, CTU in Prague, Technicka 4, 166 07, Prague 6, Czech Republic

[5]Center of Excellence Geopolymer and Green Technology (CEGeoGTech), University Malaysia Perlis, 01007 Kangar, Perlis, Malaysia

[6]School of Physical Sciences, Jawaharlal Nehru University, New Delhi 110067, India

Received: 19 February 2021 / Accepted: 28 September 2021

Abstract: In order to analyze the effect of Pd substitution on the overall electronic and magnetic properties of $L1_0$-FeNi, ab-initio calculations have been performed using density functional theory (DFT) approach within generalized gradient approximation. The magnetocrystalline anisotropy for pristine FeNi is low (< 0.5 MJ/m^3). A slight increase in its MCA is observed with single/dual substitution of Pd (from 0.430 to 0.562/0.616 MJ/m^3) as a consequence of complex spin–orbit coupling of 4*d* transition element, Pd. In the nutshell, the presence of 4*d*-element (Pd) at Fe or/and Ni sites (except FeNi:Pd_{Ni} case in which Pd substitutes only Ni) improves all the magnetic parameters including maximum energy product of $L1_0$-FeNi by appreciable amounts. In all these cases, the minimum requirement for permanent magnets, which is $H_c > M_s/2$ and $\kappa > ½$, is found to be achieved. Consequently, the Pd-substituted FeNi alloys become the potential materials for rare-earth free permanent magnets.

Keywords: Permanent magnets; DFT; FPLAPW; MCA

1. Introduction

In Ferromagnetic (FM) materials, the variations in properties of a magnetic system in accordance to the direction of the magnetization is known as the magnetic anisotropy. It is a key property for both fundamental and practical reasons for magnetic materials [1–3] and mainly consists of extrinsic and intrinsic parts. The extrinsic part is attributed by shape dependent anisotropy, related to the anisotropy in the shape of the FM materials which emerges from the famous magnetic dipole–dipole interactions [4]. On the other hand, the intrinsic part refers to magnetocrystalline anisotropy (MCA) that originates due to the collective efforts of both spin–orbit coupling (SOC) and crystal structure. The resulting orbital motion of the electrons is reserved to a particular orientation by the crystal field, and the SOC combines the same with spin degree of freedom. This means that crystal energy relies on the orientation of magnetization with respect to the crystallographic structure of materials. The origin of MCA has been a long outstanding scientific issue, and various developments have been made to advance the understanding of this phenomenon. For example, the MCA is initially due to the fact of orbital localization which is the outcome of decreased dimensionality [5, 6]. Also, the MCA is strongly influenced by SOC of the states in the environs of Fermi level (E_F). As a consequence, tailoring of the electronic band structure near the E_F determines the several crucial properties of FM materials, being responsible for tunning of MCA. This can be tuned easily by doping, adding impurities, [7–9] engineering the materials interfaces [10]. The control of this sensitive quantity can be crucial in many applications like

*Corresponding author, E-mail: manishdft@gmail.com; mkkashyap@mail.jnu.ac.in

Published online: 25 October 2021

permanent magnets (PMs) [11], magneto-optics [12] and magneto-resistive random access memory devices [13]. Currently, the rare-earth (Sm, Tb, Nd and Dy) and heavy transition-metal (Pd and Pt) based materials have large value of MCA. However, due to their limited resources and supplies along with economic and geopolitical issues, there is a need to find some alternative ferromagnetic materials with significant value of MCA [14–17].

The $L1_0$-FeNi alloy, also known as tetrataenite, is an important member for development of high performance magnets based on transition-metals [18–21] and has high MCA due to its exciting magnetic properties, large theoretically possible maximum energy product ($(BH)_{max}$ = 446 kJ/m^3), high saturation magnetization (M_s = 1.5 T), quite high Curie temperature (T_C = 830 K), high uniaxial (MCA = 1 MJ/m^3) and narrow magnetization damping constant. The formation of $L1_0$-FeNi phase exists in meteorites, where it is formed over years under exotic pressure/temperature conditions. The feeble atomic mobility makes it extremely challenging to fabricate this phase under the chemically order/disorder transition temperature (593 K) [22], Therefore, in order to fabricate artificially the same phase, distinct strives were suggested; (i) deposition of Ni and Fe monoatomic layers alternately [23, 24], (ii) high energy neutron irradiation [19], (iii) inducing epitaxial strain via suitable templates [25–27] and (iv) addition/substitution of a third element [8, 9, 28]. From previous studies, it is observed that in $L1_0$-FeNi, the main contribution to MCA comes from Fe atoms only. Further, MCA enhances by increasing ratio (c and a corresponding to the cubic out-plane and in-plane lattice parameters) of unit cell of $L1_0$-FeNi.

Theoretically, Miuara et al. [29] depicted the origin of MCA and explored the variations in MCA of $L1_0$-FeNi by varying lattice parameters(a) and reported that the MCA escalades by diminishing 'a', thus, attains a maximum at 1.6 MJ/m^3 corresponding to a = 2.250 Å (c/a = 1.75) using first-principles density functional calculations. However, experimentally, Mizuguchi et al. [19] reported the increase in MCA of $L1_0$-FeNi with escalating axial ratio c/a. Previously, our group examined the MCA of pristine and Pt doped $L1_0$-FeNi [8] and found that with a 12.5% substitutional doping of Pt, MCA increases from 0.43 to 1.37 MJ/m^3 due to tetragonal distortion (c/a = 1.433) and SOC of heavy transition-metal element, Pt. Further, $L1_0$-type FePd alloy has large MCA due to the tetragonal symmetry, and hence, it has also been extensively studied as one of the promising magnetic materials [30–33]. In this present work, we firstly plan to investigate the T_C of pristine $L1_0$-FeNi and then focus on the possible enhancement of MCA for pristine case by dilute substitutional doping of Pd. Although Pd is expensive, the purpose of our study is to add one more flavor to its extraordinary essence that it can also enhance MCA when used as a substitutional dopant via theoretical study.

2. Computational detail

For all calculations, we take the advantage of full potential linearized augmented plane wave (FPLAPW) method as implemented in WIEN2k [34] under the framework of density functional theory DFT) for calculating the electronic and magnetic properties of both pristine and optimized Pd-substituted FeNi. On Pd-substitution, the optimizations of crystal structures were obtained by lattice movement and relaxation of all the atoms using projector augmented wave (PAW) method as implemented in Vienna ab-initio simulation package (VASP) [35]. For exchange–correlation energy, we selected the Perdew, Burke and Ernzerhof (PBE) parametrization [36]-based spin dependent generalized-gradient-approximation (GGA). Further, a fully relativistic treatment was adopted for the core states whereas a scalar relativistic approach was used for the valence states. Additionally, inside the muffin-tin (MT) spheres valence electronic wavefunctions were expanded up to l_{max} = 10. In the FPLAPW calculations, the energy threshold between core and valence states was set as − 6.0 Ry. For MCA calculations of pristine FeNi, the value of radii of MT sphere (R_{MT}) was set to 2.18 a_0 for both Fe and Ni atoms, where a_0 is Bohr radius, with $R_{MT}k_{max}$ = 8. Further, in the interstitial region, G_{max} = 12 a.u.$^{-1}$ was used for Fourier expansion of potential. The modified tetrahedron method [37] was taken up for k-space integration, and a dense k-mesh of 59 × 59 × 42 (∼ 150,000 k-points in whole brillouin zone) was used for obtaining high resolution in MCA calculations of $L1_0$-FeNi. The charge and energy convergence criteria were set to be 10^{-6} e and 10^{-6} Ry, respectively.

The MCA and orbital magnetic moments are the relativistic effects, thus, the SOC Hamiltonian, H_{SO} [38] having contributions from each atomic site (i) with SOC constant, ξ_i is given by:

$$H_{SO} = \sum_i \xi_i L.S \tag{1}$$

where L and S are the single-electron angular and spin momentum operator, respectively. It was incorporated in the calculations as a second-order perturbation to the total energy and yields the following change in ground state energies of system [39]:

$$\Delta E_{SO}^{(2)} = -\sum_{n,\sigma}^{occ.} \sum_{n',\sigma'}^{unocc.} \frac{|\langle n,\sigma|H_{SO}|n',\sigma'\rangle|^2}{E^0_{n',\sigma'} - E^0_{n,\sigma}} \tag{2}$$

where $|n,\sigma\rangle$ is an unperturbed state of energy band n and

spin σ. The MCA was calculated using the magnetic force theorem [40, 41] with the formula:

$$\mathrm{MCA} = E_{100} - E_{001} \tag{3}$$

where E_{100} and E_{001} are the accumulated occupied band energy eigenvalues for magnetization vector oriented along [100] and [001] directions, respectively. Generally, the MCA constant (K) is calculated as MCA energy per unit volume, and its positive/negative indicates uniaxial/inplane MCA. For practical uses, the magnetic materials must have enough value of T_C, well above the room temperature to maintain intrinsic magnetic properties. In this direction, the estimation of T_C was made within mean field approximation (MFA) by calculating interatomic exchange coupling constants appearing in the expression of the Heisenberg Hamiltonian [42],

$$H_{\mathrm{ex}} = -\sum_{i \neq j} J_{ij} \overrightarrow{S_i} . \overrightarrow{S_j} \tag{4}$$

where S_i represents the local spin magnetic moment of the ith site, and J_{ij} stands for the exchange coupling constant among ith and jth sites.

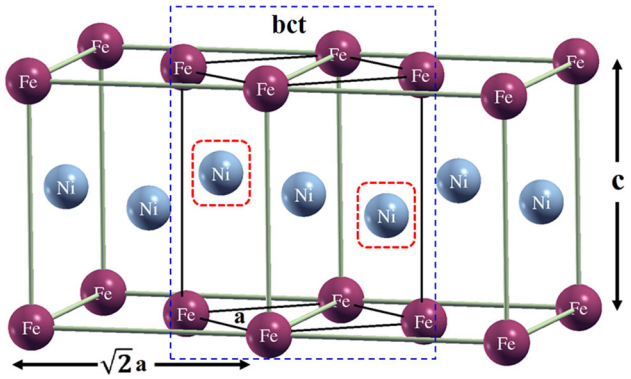

Fig. 1 Equivalent fct and bct unit cell of $L1_0$-FeNi. Note that Ni atoms shown in red dotted box are not the part of bct unit cell

3. Results and discussions

FeNi exists in tetragonal $L1_0$-structure which contains alternating atomic layers of Fe and Ni, stacked alternatively along the c-axis (spacegroup: P4/*mmm*) [43]. It can be represented by two kinds of unit cells, (i) face centered tetragonal (fct) and (ii) body centered tetragonal (bct). This type of consideration has also been used by Edström et al. [18] The bct unit cell as the input structure for the simulations is preferred due to its smallest basis that requires low computational cost [21]. In present study, we also proceeded with bct unit cell (Fig. 1) which is encompassed in two fct unit cells. Here, Fe and Ni atom are presented at (0, 0, 0) and (0.5, 0.5, 0.5), respectively. The experimental lattice parameters of $L1_0$-FeNi are a = 2.533 ± 0.002 Å and c = 3.582 ± 0.002 Å [43].

The total and atomic projected density of states of pristine $L1_0$-FeNi has already been reported previously by our group [9]. In that work, we showed that the contribution of Fe (2.70 μ_B) is larger than that of Ni (0.64 μ_B) to the total spin magnetic moment of FeNi (3.27 μ_B). Also, the calculated MCA per unit volume (K) of FeNi within GGA only was found to be 0.430 MJ/m^3. Further, the figure of merit for PMs i.e., maximum energy product ($(BH)_{max}$) for FeNi is limited due to $H_c < M_s/2$ and is 432 kJ/m^3 that defines their magnetic quality. The value of $(BH)_{max}$ [44] can be estimated by

$$(\mathrm{BH})_{\max} = \begin{cases} \frac{\mu_0 M_s^2}{4}, & H_c > M_s/2 \\ \frac{\mu_0 M_s H_c}{2}, & H_c < M_s/2 \end{cases} \tag{5}$$

In order to calculate the T_C, we considered the fct unit cell of FeNi [9] in three different magnetic configurations as shown in Fig. 2. The value of $T_C = 2J/3k_B$ [45], where, $J = \sum J_{ij}$ and k_B is Boltzmann constant, comes out to be 865 K, which is in agreement with the previous reported data (916 K [18], 823 K [46] and 830 K [47]).

The value of MCA of $L1_0$-FeNi is low, and insufficient for the use of FeNi in the PMs. Keeping this in mind, we tried to enhance its MCA by substitution of Fe or/and Ni by 4*d*-element Pd as illustrated in Fig. 3. The FeNi:$Pd_{Fe/Ni}$

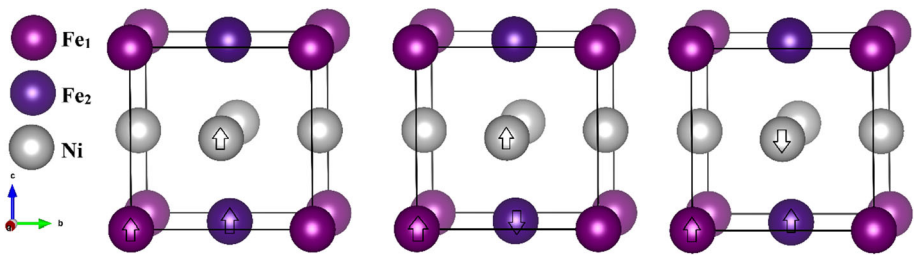

Fig. 2 (a) Ferromagnetic (FM), (b) mixed antiferromagnetic (AFM1) and (c) layered antiferromagnetic (AFM2), spin magnetic configurations of fct FeNi

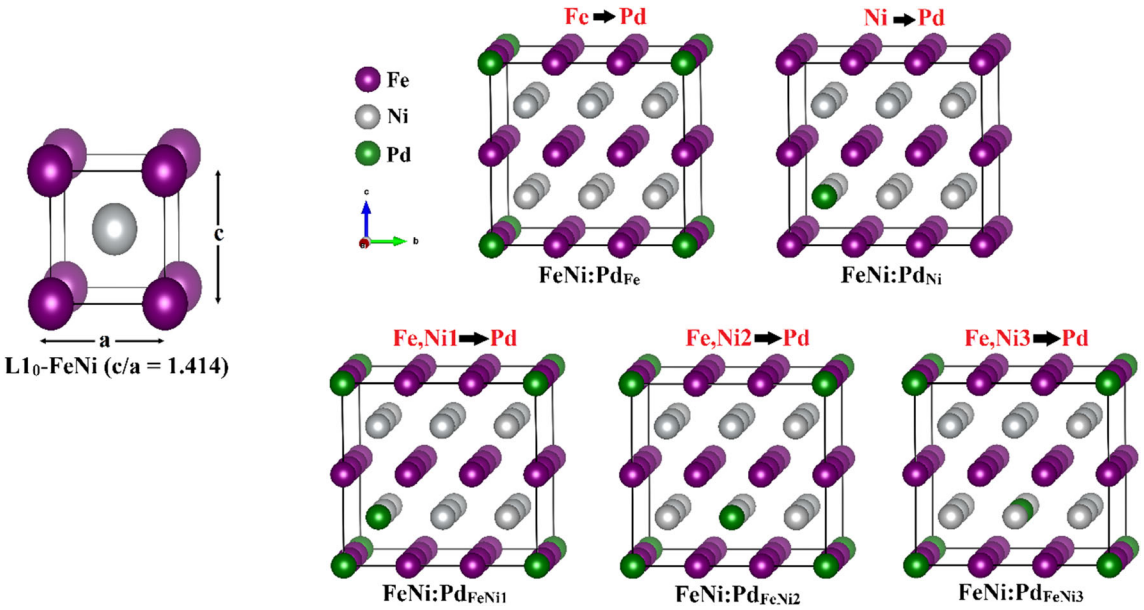

Fig. 3 $3 \times 3 \times 2$ supercell of $L1_0$ structured Pd substituted FeNi alloys. Single substitution at (a) Fe-site, (b) at Ni-site, dual substitution (c) at Fe and Ni1 sites, (d) at Fe and Ni2 sites and (e) at Fe and Ni3 sites

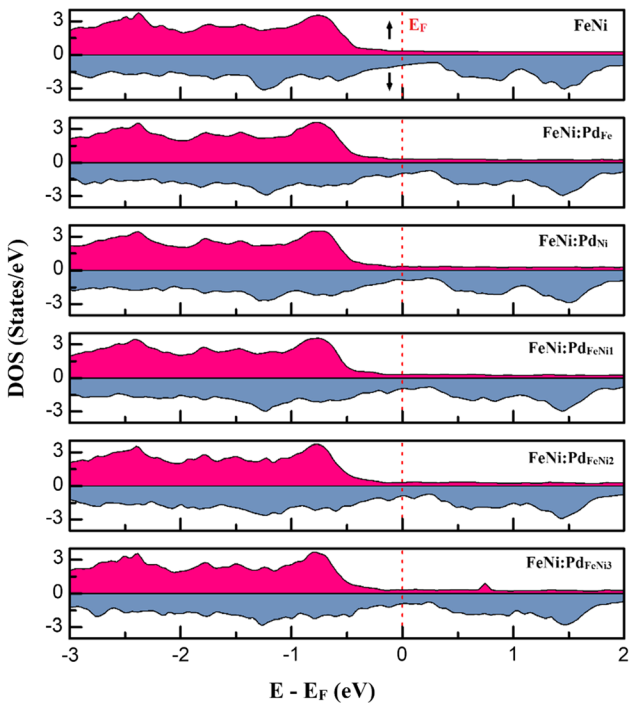

Fig. 4 Calculated spin polarized total DOS of pristine FeNi and FeNi:Pd alloys

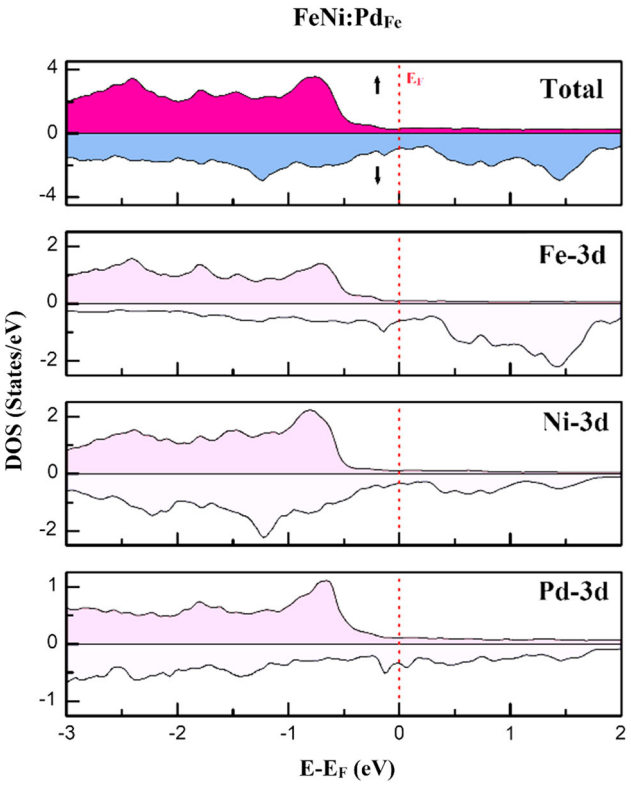

Fig. 5 Calculated spin polarized total and various *d*-orbitals DOS of FeNi:Pd$_{Fe}$ alloy

represents the substitution of one Fe/Ni by Pd in $3 \times 3 \times 2$ supercell (2.78%) of $L1_0$-FeNi and FeNi:Pd-$_{FeNi1/2/3}$ stands for dual substitution i.e., one for Fe at (0,0,0) and another for Ni which is present as first/second/third nearest neighbour of Fe by Pd in same $3 \times 3 \times 2$ supercell (5.56%).

The total density of states (DOS) in FeNi and FeNi:Pd alloys are depicted in Fig. 4. All of these DOS are spin

Table 1 Lattice parameters (a and c), tetragonal distortion (c/a), total spin magnetic moments (m_{stot}), saturation magnetization (M_s), MCA (K), coercivity (H_c), maximum energy product ($(BH)_{max}$) and magnetic hardness parameter (κ) of FeNi:Pd alloys

Alloy	(Å)	c (Å)	c/a	m_{stot} (μ_B)	M_s (T)	K (MJ/m^3)	H_c (MA/m)	$(BH)_{max}$ (KJ/m^3)	κ
FeNi	2.531*	3.579*	1.414*	3.270*	1.330*	0.430*	0.520*	432*	0.44
	2.533 ± 0.002[a]	3.582 ± 0.002[a]	–	–	–	–	–	–	–
$FeNi:Pd_{Fe}$	2.521	3.585	1.422	3.163	1.615	0.562	0.694	520	0.66
$FeNi:Pd_{Ni}$	2.522	3.592	1.424	3.271	1.665	0.502	0.604	501	0.61
$FeNi:Pd_{FeNi1}$	2.533	3.602	1.422	3.163	1.592	0.554	0.694	505	0.66
$FeNi:Pd_{FeNi2}$	2.532	3.603	1.423	3.169	1.596	0.588	0.735	508	0.68
$FeNi:Pd_{FeNi3}$	2.532	3.603	1.423	3.171	1.596	0.616	0.770	508	0.70

*Ref. [9], [a]Ref [43]

polarized, indicating the ferromagnetic behavior for all. With substitution of Pd in place of Fe or/and Ni in FeNi, no significant change is observed. To analyze the states responsible for total DOS, the contributions from d-orbitals of all three transition metals (Fe, Ni and Pd) in $FeNi:Pd_{Fe}$ configuration have been displayed in Fig. 5. For brevity, only one configuration ($FeNi:Pd_{Fe}$) is discussed and for all other studied configurations, same explanation is expected. From Fig. 5, it is clear that all d-DOS of Fe-, Ni- and Pd-atoms equally contributing in total DOS, suggestion strong d-d coupling among all three.

The tetragonal distortion (c/a) and magnetic properties of FeNi:Pd alloys, as listed in Table 1, indicate that the value of c/a increases slightly on substitution of Fe or/and Ni by Pd due to relatively larger size of 4d-element (Pd) as compared to that of 3d-elements (Fe and Ni). Further, our calculations reveal that the saturation magnetization decreases on replacement of Fe or/and Ni by Pd which is an expected behavior due to low magnetic moment of Pd ($\sim$ 0.37 μ_B) as compared to that of Fe ($\sim$ 2.69 μ_B) and Ni ($\sim$ 0.69 μ_B).

In case of $FeNi:Pd_{Ni}$, total spin magnetic moment remains almost same because here, Ni ($3d^8$) is substituted by Pd ($4d^8$) element having similar valence d-configuration. For all FeNi:Pd alloys, MCA increases as compared to pristine FeNi. This increase is clearly a consequence of tetragonal distortion induced due to the involvement of large sized 4d-element (Pd). Although the tetragonal distortion is almost same in all FeNi:Pd alloys for dual substitutions (Table 1), however, the MCA enhances as the nearest neighbor (n–n) distance between Pd substitutions at Fe-site (0,0,0) and Ni-site increases. Further, there is only a slight increase in MCA with single/dual substitution of Pd (from 0.430 to 0.562/0.616 MJ/m^3). Besides tetragonal distortion effect, this kind of complicated behavior of MCA with Pd substitution may be related complex SOC of 4d transition element, Pd.

The value of coercivity (H_c), maximum energy product ($(BH)_{max}$) and magnetic hardness parameter, $\kappa = \sqrt{K/\mu_0 M_s^2}$, for studied alloys are listed in Table 1. Our estimated H_c follows the same trend as that of MCA, however, for all substituted alloys except $FeNi:Pd_{Ni}$, the minimum requirement for PMs, which is $H_c > M_s/2$ and $\kappa > ½$, has been attained [48]. Moreover, $(BH)_{max}$ also gets increased for all the cases which is an advantageous property for PMs. Therefore, the FeNi:Pd alloys are conceivable candidates with optimum properties for the application in PMs.

4. Conclusions

In quest for finding the materials free from rare-earth and critical transition-metal elements with significant magnetocrystalline anisotropy, we have investigated the Pd-substituted $L1_0$-FeNi alloys via density functional theory-based full potential simulations. Our calculated results for FeNi:Pd alloys (except $FeNi:Pd_{Ni}$) predict that dilute Pd-substitutional doping offers an ideal platform for realizing the minimum hard magnetic properties to achieve the technological applications i.e., large magnetization with optimum uniaxial magnetic anisotropy, coercivity and hardness parameter. A slight increase in MCA of FeNi with single/dual substitution of Pd (from 0.430 to 0.562/0.616 MJ/m^3) is observed which is a consequence of complex spin–orbit coupling of 4d transition element, Pd. We hope that our predictions will inspire the experimentalists towards rare-earth free high performance permanent magnetic and spintronic materials based on FeNi:Pd alloys.

Acknowledgments The computation in this work was performed using Param Shavak supercomputing machine available at Department of Physics, Kurukshetra University, Kurukshetra (Haryana) and the National PARAM Supercomputing Facility (NPSF) of Center for Development of Advanced Computing (C-DAC), Pune, India. P. Rani

and M. K. Kashyap acknowledge DST-SERB, New Delhi, for providing financial assistantship vide Grant No. EMR/2016/007380.

References

[1] J Stöhr and H C Siegmann *Magnetism Solid State Sciences Series*. (Berlin: Springer) (2006)
[2] Y Kota and A Sakuma *J. Phys. Soc. Jpn.* **83** 034715 (2014).
[3] A Sakuma *J. Phys. Soc. Jpn.* **63** 3053 (1994).
[4] G H O Daalderop, P J Kelly and M F H Schuurmans *Phys. Rev. B* **41** 11919 (1990).
[5] J M D Coey *Magnetism and Magnetic Materials*. (Cambridge: Cambridge University Press) (2010)
[6] P Bruno and J P Renard *Appl. Phys. A* **49** 499 (1989).
[7] D Odkhuu and S C Hong *Phys. Rev. Appl.* **11** 054085 (2019).
[8] P Rani, J Thakur, A Taya and M K Kashyap *Vacuum* **159** 186 (2019).
[9] P Rani, M K Kashyap, R Singla, J Thakur and A H Reshak *J. Alloys Compd.* **835** 155325 (2020).
[10] K Nakamura, T Akiyama, T Ito, M Weinert and A J Freeman *Phys. Rev. B* **81** 220409 (2010).
[11] K D Belashchenko and V P Antropov *Phys. Rev. B* **66** 144402 (2002).
[12] V N Antonov, V P Antropov, B N Harmon, A N Yaresko and A Y Perlov *Phys. Rev. B* **59** 14552 (1999).
[13] J M Hu, Z Li, L Q Chen and C W Nan *Nat. Commun.* **2** 1 (2011).
[14] H Kronmüller *J. Magn. Magn. Mater.* **140** 25 (1995).
[15] N Jones *Nature* **472** 22 (2011).
[16] J Cui, M Kramer, L Zhou, F Liu, A Gabay, G Hadjipanayis, B Balasubramanian and D Sellmyer *Acta Mater.* **158** 118 (2018).
[17] J M D Coey *IEEE Trans. Magn.* **47** 12 4671 (2011).
[18] A Edström, J Chico, A Jakobsson, A Bergman and J Rusz *Phys. Rev. B* **90** 014402 (2014).
[19] M Mizuguchi, T Kojima, M Kotsugi, T Koganezawa, K Osaka and K Takanashi *J. Magn. Soc. Jpn.* **35** 370 (2011).
[20] E Poirier et al *J. Appl. Phys.* **117** 17E318 (2015).
[21] M Ogiwara et al. *Appl. Phys. Lett.* **103** 242409 (2013)
[22] I G Kabanova, V V Sagaradze and N V Kataeva *Phys. Metals Metallogr.* **112** 267 (2011).
[23] T Shima, M Okamura, S Mitani and K Takanashi *J. Magn. Magn. Mater.* **310** 2 2213 (2007).
[24] T Kojima et al *J. Phys. Condens. Matter* **26** 064207 (2014).
[25] T Kojima, M Mizuguchi and K Takanashi *Thin Solid Films* **603** 348 (2015).
[26] A Frisk, T P Hase, P Svedlindh, E Johansson and G Andersson *J. Phys. D Appl. Phys.* **50** 085009 (2016).
[27] T Kojima, M Mizuguchi and K Takanashi *J. Phys. Conf. Ser.* **266** 012119 (2011).
[28] T Kojima et al *J. Phys. D Appl. Phys.* **47** 425001 (2014).
[29] Y Miura, S Ozaki, Y Kuwahara, M Tsujikawa, K Abe and M Shirai *J. Phys. Condens. Matter* **25** 106005 (2013).
[30] D Ravelosona, A Cebollada, F Briones, C Diaz-Paniagua, M A Hidalgo and F Batallan *Phys. Rev. B* **59** 4322 (1999).
[31] O Klein et al *J. Appl. Phys.* **89** 6781–6783 (2001).
[32] P R Aitchison et al *J. Magn. Magn. Mater.* **223** 138 (2001).
[33] K Chesnel et al *Phys. Rev. B* **66** 172404 (2002).
[34] P Blaha, K Schwarz, G K Madsen, D Kvasnicka and J Luitz *WIEN2k. An augmented plane wave+ local orbitals program for calculating crystal properties* (2001)
[35] G Kresse and J Furthmüller *Phys. Rev. B* **54** 11169 (1996).
[36] J P Perdew, K Burke and M Ernzerhof *Phys. Rev. Lett.* **77** 3865 (1996).
[37] P E Blöchl, O Jepsen and O K Andersen *Phys. Rev. B* **49** 16223 (1994).
[38] R Wu and A J Freeman *J. Magn. Magn. Mater.* **200** 498 (1999).
[39] P Bruno *Phys. Rev. B* **39** 865 (1989).
[40] A R Mackintosh and O K Andersen *Electrons at the Fermi Surface*, (London: Cambridge University Press), *Ed. M. Springford* 149 (1980)
[41] H J F Jansen *J. Appl. Phys.* **67** 4555 (1990).
[42] R F Evans, W J Fan, P Chureemart, T A Ostler, M O Ellis and R W Chantrell *J. Phys. Condens. Matter* **26** 1202 (2014).
[43] R S Clarke and E R Scott *Am. Mineral.* **65** 624 (1980).
[44] R Skomski and J M D Coey *Phys. Rev. B* **48** 15812 (1993).
[45] L M Sandratskii and P Bruno *J. Phys. Condens. Matter* **15** 585 (2003).
[46] P Wasilewski *Phys. Earth Planet. Inter.* **52** 150 (1988).
[47] L H Lewis et al. *J. Phys. Condens. Matter* **26** 064213 (2014)
[48] R Skomski and J M D Coey *Permanent Magnetism*. (London: Routledge) (2019)